Macromodeling of microwave structures based on noisy frequency-domain data

D. Deschrijver, T. Dhaene [1]

Abstract: Frequency-domain macromodeling tools are of paramount importance for the design and study of microwave structures. In this paper, a reliable identification method, called Orthormal Vector Fitting method, is combined with a relaxation constraint. This leads to more accurate fitting models, in a limited amount of computation time, especially if the spectral data is contaminated with noise. Its performance is analyzed on a measurement-based example and compared to other existing approaches in the field.

1 Introduction

Vector Fitting (VF) is a robust identification method which characterizes the spectral response of passive structures quite accurately [1]. It has been widely applied as a macromodeling tool for the design and analysis of microwave structures. The method is essentially the combination of a partial fraction basis and an iterative least-squares framework. In [2], the numerical stability of the VF method was improved by using orthonormal rational functions instead of partial fractions. This has lead to the Orthonormal Vector Fitting (OVF) method [3]. In [4], the accuracy of the method was improved for noisy frequency domain data, and has lead to the Relaxed Vector Fitting (RVF) method. In this paper, the benefits of both methods are combined, leading to ROVF [5], and are illustrated by a measurement-based example.

2 Non-linearity of the approximation problem

A rational transfer function $R(s)$ is defined as a quotient of two polynomials $N(s)$ and $D(s)$. The numerator and denominator of the transfer function can be represented as a linear combination of P orthonormal rational functions ϕ_p.

$$R(s) = \frac{N(s)}{D(s)} = \frac{\sum_{p=1}^{P} c_p \phi_p(s,a)}{\tilde{c}_0 + \sum_{p=1}^{P} \tilde{c}_p \phi_p(s,a)} \qquad s = i2\pi f \tag{1}$$

The denominator has an additional basis function which equals the constant value 1, and the coefficients c_p and $\tilde{c}_p$ represent the model coefficients. $\phi_p(s,a)$ represents the p^{th} orthonormal rational basis function, based on a prescribed set of poles $a = \{-a_1, ..., -a_P\}$, and evaluated at complex frequency s. Given a set of Laplace data samples $(s_k, H(s_k))$, the transfer function should match the data in a least squares sense, such that $R(s_k) \simeq H(s_k)$, for $k = 0, ..., K$.

The numerator and denominator can be factorized as follows

$$N(s) = \sum_{p=1}^{P} c_p \phi_p(s,a) = \frac{\prod_{p=1}^{P-1}(s + z_{p,n})}{\prod_{p=1}^{P}(s + a_p)} \tag{2}$$

$$D(s) = \tilde{c}_0 + \sum_{p=1}^{P} \tilde{c}_p \phi_p(s,a) = \frac{\prod_{p=1}^{P}(s + z_{p,d})}{\prod_{p=1}^{P}(s + a_p)} \tag{3}$$

and the transfer function $R(s)$ is obtained as

$$R(s) = \frac{N(s)}{D(s)} = \frac{\prod_{p=1}^{P-1}(s + z_{p,n})}{\prod_{p=1}^{P}(s + z_{p,d})} = \sum_{p=1}^{P} \alpha_p \phi_p(s, z_d) \tag{4}$$

In the first iteration step ($t = 0$), Levi's estimator is applied to obtain a first guess of the denominator [6]. The initial poles of the basis functions are chosen to be a set of prescribed poles a. The coefficients $c_p^{(0)}$ and $\tilde{c}_p^{(0)}$ of $N(s)$ and $D(s)$ are calculated by minimizing following cost function

$$\arg \min_{\tilde{c}_p^{(t)}, c_p^{(t)}} \left(\sum_{k=0}^{K} \left| D^{(0)}(s_k) H(s_k) - N^{(0)}(s_k) \right|^2 \right) \tag{5}$$

[1] Computer Modeling and Simulation, Department of Mathematics and Computer Science, University of Antwerp, Middelheimlaan 1, 2020 Antwerp, Belgium. Email: dirk.deschrijver@ua.ac.be, tom.dhaene@ua.ac.be

$$= \arg\min_{\tilde{c}^{(0)},c^{(0)}} \left(\sum_{k=0}^{K} \left| \left(\sum_{p=1}^{P} \tilde{c}_p^{(0)} \phi_p(s_k, a) + \tilde{c}_0^{(0)} \right) H(s_k) - \sum_{p=1}^{P} c_p^{(0)} \phi_p(s_k, a) \right|^2 \right) \quad (6)$$

Then the Sanathanan-Koerner linearization can be applied to relieve the bias of Levi's estimator, for iteration step $t = 1, ..., T$ [7]

$$\arg\min_{\tilde{d}^{(t)},d^{(t)}} \left(\sum_{k=0}^{K} \left| \frac{1}{D^{(t-1)}(s_k)} \right|^2 \left| D^{(t)}(s_k) H(s_k) - N^{(t)}(s_k) \right|^2 \right) \quad (7)$$

$$= \arg\min_{\tilde{d}^{(t)},d^{(t)}} \left(\sum_{k=0}^{K} \left| \left(\sum_{p=1}^{P} \tilde{d}_p^{(t)} \phi_p(s_k, z_d^{(t-1)}) + \tilde{d}_0^{(t)} \right) H(s_k) - \sum_{p=1}^{P} d_p^{(t)} \phi_p(s_k, z_d^{(t-1)}) \right|^2 \right) \quad (8)$$

In these successive iteration steps ($t > 0$), the coefficients $\tilde{d}_p^{(t)}$ of $D^{(t)}(s)/D^{(t-1)}(s)$ are used to calculate the relocated poles of the transfer function. This doesn't pose a problem, as the zeros of $D^{(t)}(s)$ and $D^{(t)}(s)/D^{(t-1)}(s)$ are the same. By analyzing the gradients of the error criterion, it can be shown that (7) does not converge to the true least squares solutions, even though the error criterion itself tends asymptotically to the fundamental least squares criterion [8]. In practice, however, this approach often gives favorable results for sufficiently high signal-to-noise ratios and sufficiently small modeling errors. When fitting noisy frequency data however, the SK-linearization can fail to relocate the poles properly. In order to alleviate this problem, a relaxation constraint can be applied.

3 Relaxation constraint

In order to avoid the trivial null solution in (5) and (7) , one coefficient e.g. $\tilde{d}_0$ is fixed to unity. This can be done without loss of generality since both numerator and denominator can be divided by the same constant value. It should be noted that this choice can seriously compromise the conditioning of the normal equations, especially if the true value of this coefficient is 0, or close to 0.

In [4], a relaxation constraint is introduced which improves the normalization of the coefficients of the transfer function, and the linearization of the SK-iteration at the same time. These difficulties can be alleviated by introducing a more relaxed non-triviality constraint as an additional row in the system matrix. This constraint imposes that the sum of the denominator samples approaches a non-zero value without fixing any of its coefficients.

$$\Re e \left\{ \sum_{k=0}^{K} \left(\sum_{p=1}^{P} \tilde{d}_p^{(t)} \phi_p(s_k, z_d^{(t-1)}) + \tilde{d}_0^{(t)} \right) \right\} = K + 1 \quad (9)$$

This equation is given a LS weighting in relation to the size of H.

$$weight = \|w(s)H(s)\| / (K + 1) \quad (10)$$

4 Example : Microstrip Lines

A 6 inch coupled microstrip lines on an FR4 PC board was measured [9], and the reflection coefficient S_{11} is approximated over the frequency range [0.05 GHz - 20 GHz] by an 80-pole, proper transfer function. The magnitude and the phase of the data are shown in Figure 1 and Figure 2.

First a prescribed set of 80 conjugate starting poles are chosen on a straight line, close to the imaginary axis, according to the following pole-location scheme

$$-a_p = -\alpha + \beta i, -a_{p+1} = -\alpha - \beta i \quad (11)$$

$$\alpha = v\beta_{\max} \quad (12)$$

with imaginary parts β covering the frequency range of interest, and v set to 1 and 0.01 respectively. In this example, all frequencies are scaled by 10^9.

The VF, OVF, RVF and ROVF methods are used to relocate these poles, in order to minimize the fitting error. Unstable poles are flipping into the left-half plane during each iteration, in order to enforce stability of the poles. The RMS error is shown in terms of the iteration count, in Figure 3 and 4.

If Figure 3 is considered, two interesting facts can be observed :

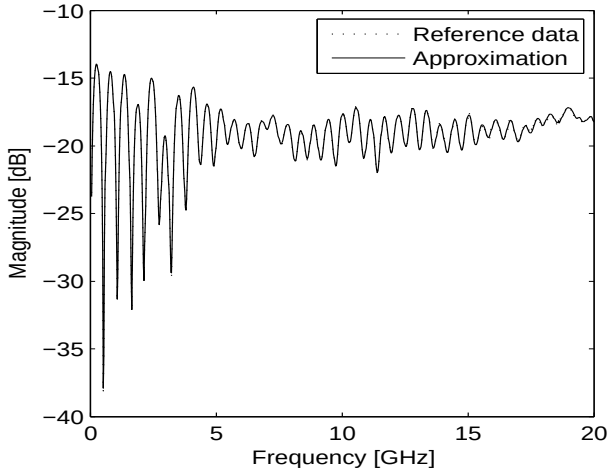

Figure 1: Magnitude S11

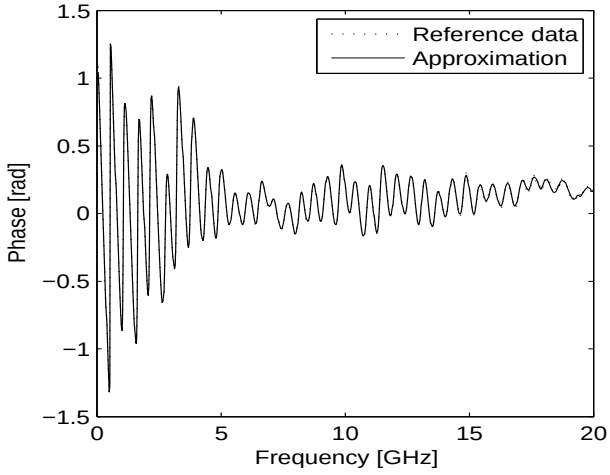

Figure 2: Phase S11

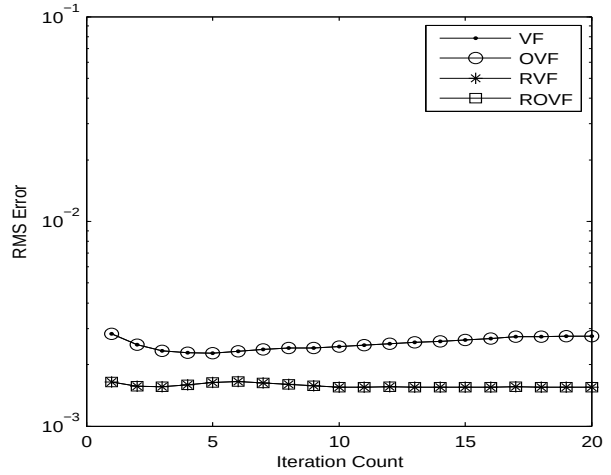

Figure 3: RMS Error vs. Iteration count (v=0.01)

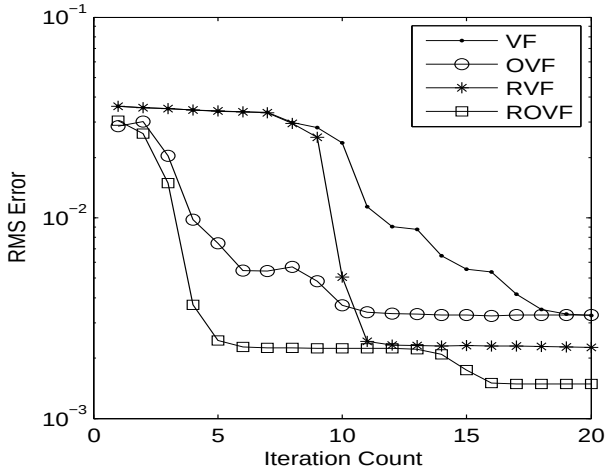

Figure 4: RMS Error vs. Iteration count (v=1)

- If the real part of the starting poles is chosen sufficiently small ($v = 0.01$), no significant difference can be observed between VF vs OVF and RVF vs ROVF. This can easily be seen by analyzing the structure of the basisfunctions. Note that the orthonormal basis functions

$$\phi_p(s) = \frac{\sqrt{2\Re e(a_p)}}{s + a_p} \left(\prod_{j=1}^{p-1} \frac{s - a_j^*}{s + a_j} \right) \tag{13}$$

  are essentially the partial fractions $(s + a_p)^{-1}$, multiplied with some all-pass functions and a normalization constant. The all-pass functions increase the phase variation of the basis functions, leading to a better numerical conditioning. If the real part of a pole, say $-a_p = 0 + i\omega_p$, has a zero real part, than the all-pass function

$$\frac{s - a_p^*}{s + a_p} = \frac{i\omega - i\omega_p}{i\omega - i\omega_p} = 1 \tag{14}$$

  simply reduces to a multiplication by 1. Consequently, the unnormalized orthogonal basis functions reduce to the partial fraction basis if the real part of the poles is chosen sufficiently small. The normalization constant simply results in a scaling of the columns of the system equations. It was already observed that this improves the conditioning of the system equations, and can lead to more accurate results. This idea was also implemented in the standard VF technique [1] by scaling the columns of the system matrix to unity length. This can also be useful for the orthonormal basis, if polynomial terms are added to the numerator, to vary the order of the transfer function.

- The fitting models which are calculated using RVF and ROVF are more accurate than the fitting models which are calculated using VF and OVF. Since the measurement data is contaminated with

noise, the SK-linearization does not converge close enough to the true least-squares solution. By adding the relaxation constraint as an additional line in the system matrix, the linearization of the non-linear problem is fundamentally changed, resulting in an improved fitting procedure. In addition, freeing up a fixed model coefficient improves the accuracy of the fitting model as well.

If Figure 4 is considered, three interesting facts can be observed :

- If the real part of the starting poles is non-negligible with respect to the true poles ($v = 1$) , then the fitting models which are calculated using the orthonormal basis (OVF and ROVF) become significantly more accurate in the first iterations. This is caused by the use of orthonormal rational functions, which improve the numerical conditioning of the system equations.
- In the final iterations, VF and OVF converge to the same result as the prescribed poles are relocated to their optimal position.
- For this example, ROVF gives more accurate results than RVF in the final iteration. In the general situation, both methods converge to similar results, however ROVF often needs less iterations. In this example, ROVF needs 5 iterations to obtain a similar accuracy as RVF in 11 iterations. This results in a $\sim$54.5% reduction of the overall computation time.

5 Conclusions

It is well-known that the use of rational basis functions, applied in an iterative least-squares framework results in a robust identification method. Orthonormal rational bases can further improve the numerical conditioning of the system equations, especially if the real part of the starting poles is non-negligible. The linearization of the SK-iteration can be improved by incorporating a relaxation constraint as an additional row in the system matrix. It was further shown that the combination of both methods provides improved fitting results.

6 Acknowledgements

This work is supported by the Fund for Scientific Research Flanders (FWO-Vlaanderen).

References

[1] B. Gustavsen and A. Semlyen, Rational Approximation of Frequency Domain Responses by Vector Fitting, IEEE Transactions on Power Delivery,14 (3), 1052-1061, 1999.

[2] D. Deschrijver and T. Dhaene, Rational Modeling of Spectral Data using Orthonormal Vector Fitting, 9th IEEE Workshop on Signal Propagation on Interconnects (SPI 2005), Garmisch-Partenkirchen (Germany), 111-114, 2005.

[3] D. Deschrijver and T. Dhaene, Broadband Macromodeling of Passive Components using Orthonormal Vector Fitting, IEE Electronic Letters, 41(2), 1160-1161, 2005.

[4] B. Gustavsen, Improving the Pole Relocating Properties of Vector Fitting, IEEE Transactions on Power Delivery, in print, 2006.

[5] D. Deschrijver, B. Gustavsen and T. Dhaene, Advancements in Iterative Methods for Rational Approximation in the Frequency Domain, IEEE Transactions on Power Delivery, submitted, 2006.

[6] E.C. Levi, Complex Curve Fitting, IEEE Transactions on Automatic Control, AC-4, 37-43, 1959.

[7] C.K. Sanathanan and J. Koerner, Transfer Function Synthesis as a Ratio of Two Complex Polynomials, IEEE Transactions on Automatic Control, AC-8, 56-58, 1963.

[8] A.H. Whitfield, Asymptotic Behavior of Transfer Function Synthesis Methods, International Journal of Control, 45, 1083–1092, 1987.

[9] W. Beyene and C. Yuan, An Accurate Transient Analysis of High-Speed Package Interconnects Using Convolution Technique, Analog Integrated Circuits and Signal Processing, 35 (2-3), 107-120, 2003.